nature cell biology

SUPPLEMENTARY INFORMATION

https://doi.org/10.1038/s41556-019-0329-y

In the format provided by the authors and unedited.

Non-canonical function of IRE1α determines mitochondria-associated endoplasmic reticulum composition to control calcium transfer and bioenergetics

Amado Carreras-Sureda[1,2,3], Fabián Jaña[2,4], Hery Urra[1,2,3], Sylvere Durand[5,6], David E. Mortenson[7], Alfredo Sagredo[1,2,3], Galdo Bustos[2,4,8], Younis Hazari[1,2,3], Eva Ramos-Fernández[9], Maria L. Sassano[10], Philippe Pihán[1,2,3], Alexander R. van Vliet[10], Matías González-Quiroz[1,2,3], Angie K. Torres[11], Cheril Tapia-Rojas[11], Martijn Kerkhofs[12], Rubén Vicente[13], Randal J. Kaufman[14], Nibaldo C. Inestrosa[9], Christian Gonzalez-Billault[2,15,16], R. Luke Wiseman[7], Patrizia Agostinis[10], Geert Bultynck[14], Felipe A. Court[2,8], Guido Kroemer[5,6,17,18,19], J. César Cárdenas[2,4,8,20] and Claudio Hetz[1,2,3,15,21]*

[1]Biomedical Neuroscience Institute, Faculty of Medicine, University of Chile, Santiago, Chile. [2]FONDAP Geroscience Center for Brain Health and Metabolism, Santiago, Chile. [3]Program of Cellular and Molecular Biology, Institute of Biomedical Sciences, University of Chile, Santiago, Chile. [4]Anatomy and Developmental Biology Program, Institute of Biomedical Sciences, University of Chile, Santiago, Chile. [5]Equipe Labellisée par la Ligue contre le cancer, Université Paris Descartes, Université Sorbonne Paris Cité, Université Paris Diderot, Sorbonne Université, INSERM U1138, Centre de Recherche des Cordeliers, Paris, France. [6]Metabolomics and Cell Biology Platforms, Institut Gustave Roussy, Villejuif, France. [7]Department of Molecular Medicine, The Scripps Research Institute, La Jolla, CA, USA. [8]Center for Integrative Biology, Faculty of Sciences, Universidad Mayor, Santiago, Chile. [9]Center for Aging and Regeneration, Department of Cell and Molecular Biology, Faculty of Biological Sciences, Pontifical Catholic University of Chile, Santiago, Chile. [10]Laboratory of Cell Death Research and Therapy, Department of Cellular and Molecular Medicine, VIB-KU Leuven Center for Cancer Biology, KU Leuven, Leuven, Belgium. [11]Laboratory of Neurobiology of Aging, Centro de Biología Celular y Biomedicina, Facultad de Medicina y Ciencia, Universidad San Sebastián, Santiago, Chile. [12]Laboratory of Molecular and Cellular Signaling, Department of Cellular and Molecular Medicine and Leuven Kanker Instituut, KU Leuven, Leuven, Belgium. [13]Laboratory of Molecular Physiology, Department of Experimental and Health Sciences, Universitat Pompeu Fabra, Barcelona, Spain. [14]Degenerative Diseases Program, Sanford Burnham Prebys Medical Discovery Institute, La Jolla, CA, USA. [15]Buck Institute for Research on Aging, Novato, CA, USA. [16]Department of Biology, Faculty of Sciences, University of Chile, Santiago, Chile. [17]Pôle de Biologie, Hôpital Européen Georges Pompidou, AP-HP, Paris, France. [18]Karolinska Institute, Department of Women's and Children's Health, Karolinska University Hospital, Stockholm, Sweden. [19]Suzhou Institute for Systems Biology, Chinese Academy of Sciences, Suzhou, China. [20]Department of Chemistry and Biochemistry, University of California, Santa Barbara, CA, USA. [21]Department of Immunology and Infectious Diseases, Harvard School of Public Health, Boston, MA, USA. *e-mail: chetz@hsph.harvard.edu

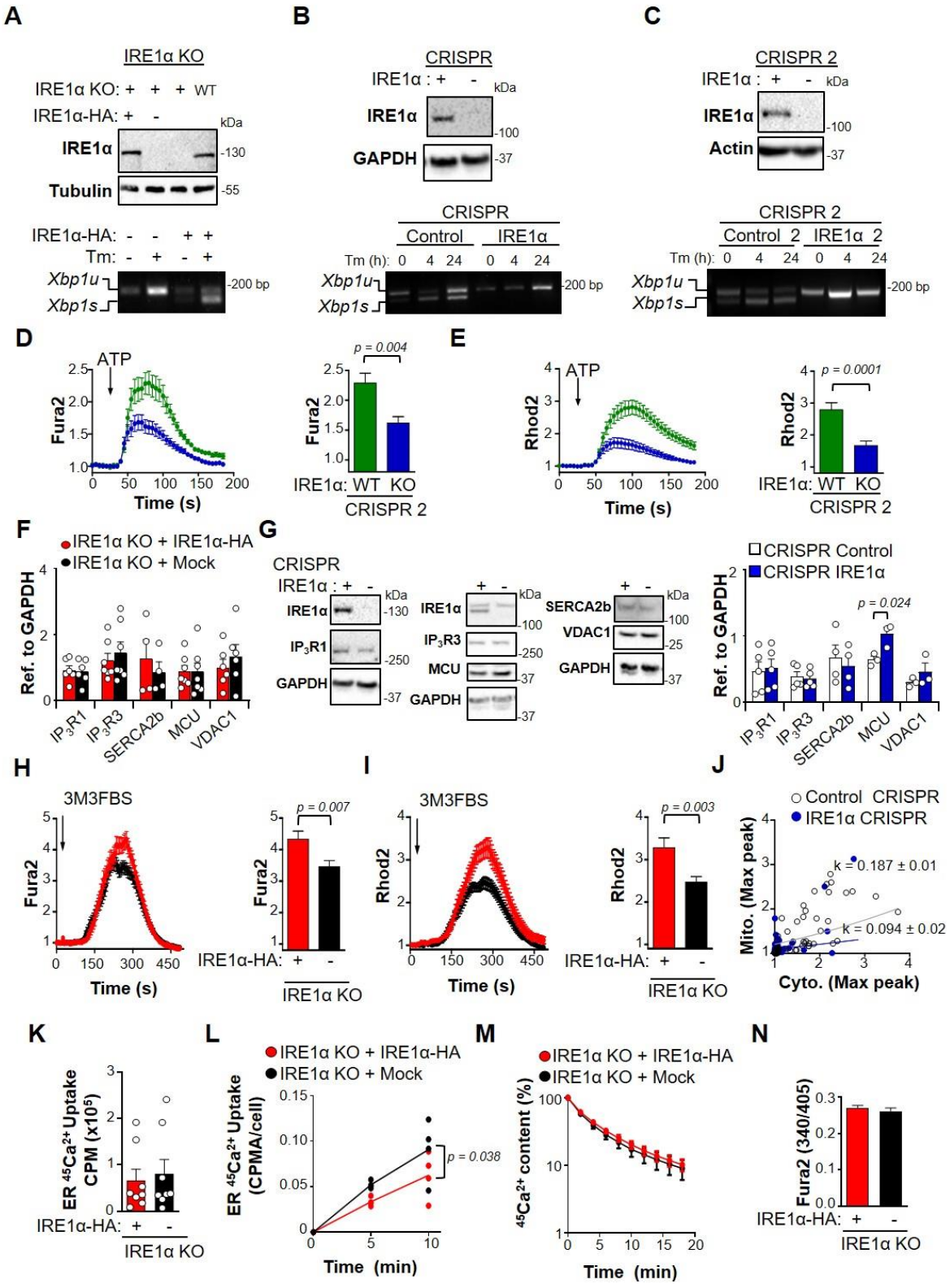

Supplementary Figure 1

IRE1α is located at MAMs and regulates ER to mitochondria communication.

(A) IRE1α-KO cells reconstituted with IRE1α-HA or empty vector (Mock), processed for (WB) for the indicated proteins. Bottom: RT-PCR for *Xbp1* mRNA splicing after 8 h of 0.5 µg/ml tunicamycin (Tm) treatment (n = 3 independent experiments). **(B)** CRISPR control and IRE1α KO cells, or an additional set of cells **(C)** were analysed as described in A (n =3 independent experiments). **(D-E)** CRISPR control and IRE1α KO (clone 2) cells imaged for calcium levels in the cytosol and mitochondria (arrow = 100 µM ATP). Right: maximum peak for normalized Fura2 were quantified (total cells analysed: Control 2: n = 45; IRE1α 2: n = 75). **(F)** WB analysis for the indicated proteins of cells described in 1G normalized to GAPDH (IP_3R1: n = 6; IP_3R3: n = 7: SERCA2b: n = 4; MCU: n = 7; VDAC1: n = 6; all n are biologically independent). **(G)** CRISPR control and IRE1α KO cells were processed as indicated in F (IP_3R1: n = 5; IP_3R3: n = 5; SERCA2b: n = 4; MCU: n = 3; VDAC1: n = 3; all n are biologically independent samples). **(H-I)** Same cells as in F were simultaneously imaged for calcium levels as in D-E (arrow = 50 µM 3M3FBS) (cells analysed: Mock: n = 93; IRE1α-HA: n = 97) **(J)** Maximum peak from Fura2/Rhod2 measurements from same samples as in Figure 1E-F calculated with non-linear regression analyses to obtain correlation constant (*K*). **(K-L)** Cells were loaded with $^{45}Ca^{2+}$ to determine ER $^{45}Ca^{2+}$ loading at steady-state levels (K, n = 8 independent experiments) or after 5-10 minutes of $^{45}Ca^{2+}$ loading (L, n = 4 independent experiments). **(M)** Unidirectional $^{45}Ca^{2+}$ efflux from the ER loaded to $^{45}Ca^{2+}$ steady-state levels. Graph displays normalized ER $^{45}Ca^{2+}$ content (%) over time (n = 8 independent experiments). **(N)** Resting Fura2-AM ratio (340/405) measurements for the indicated cell lines (cells analysed: Mock: n = 99; IRE1α-HA: n = 109). All plots represent mean and SEM. Statistical differences were detected with unpaired two-tail Student´s t-test or Two-way ANOVA (L). Source data have been provided in Supplementary Table 6.

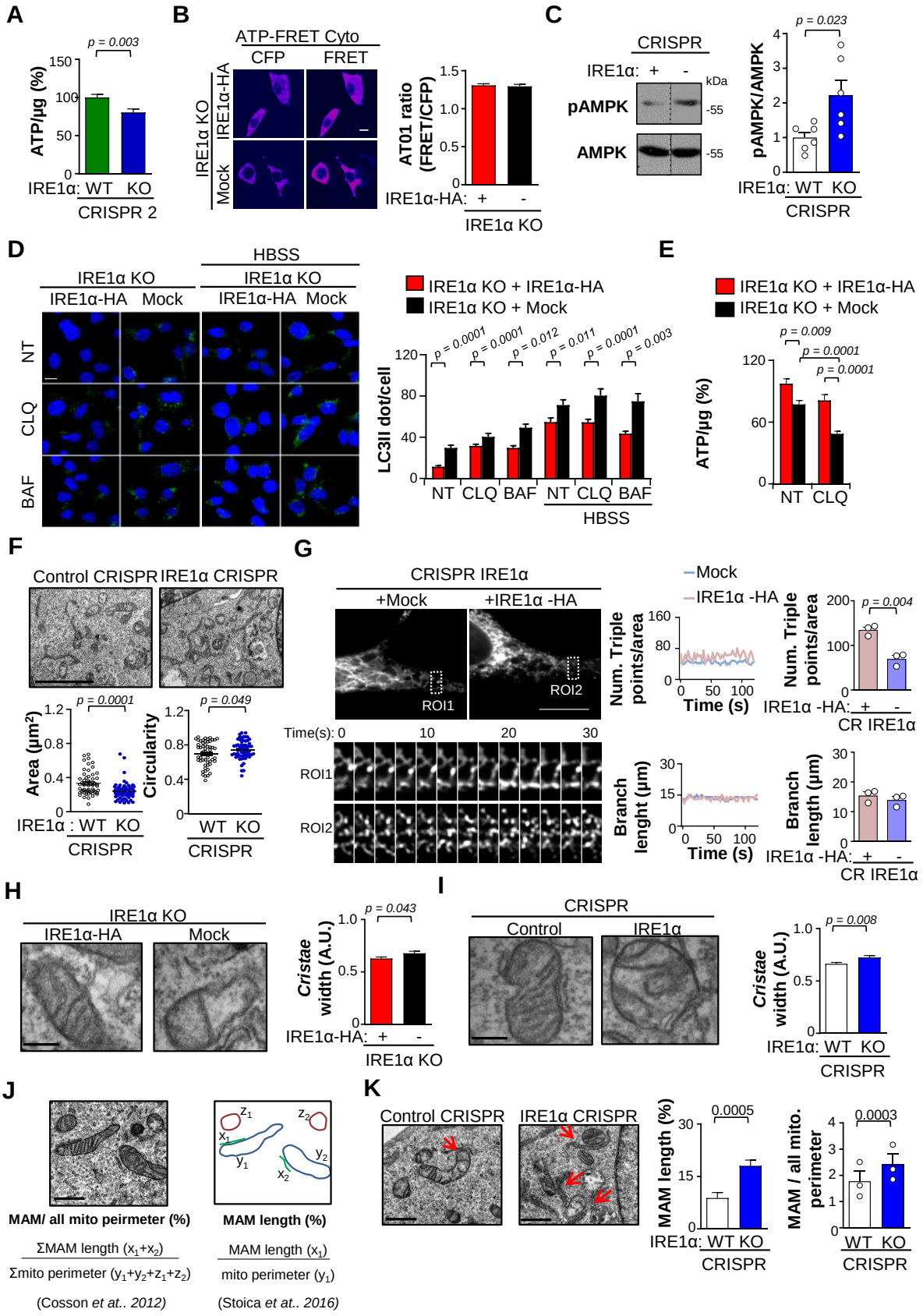
A
ATP/µg (%)
p = 0.003
IRE1α: WT KO
CRISPR 2
B
ATP-FRET Cyto
CFP
FRET
IRE1α KO
IRE1α-HA
Mock
AT01 ratio (FRET/CFP)
IRE1α-HA: + -
IRE1α KO
C
CRISPR
IRE1α: + -
kDa
pAMPK
AMPK
-55
pAMPK/AMPK
p = 0.023
IRE1α: WT KO
CRISPR
D
HBSS
IRE1α KO
IRE1α-HA Mock
NT
CLQ
BAF
IRE1α KO + IRE1α-HA
IRE1α KO + Mock
LC3II dot/cell
p = 0.0001
p = 0.0001
p = 0.012
p = 0.011
p = 0.0001
p = 0.003
NT CLQ BAF NT CLQ BAF
HBSS
E
IRE1α KO + IRE1α-HA
IRE1α KO + Mock
ATP/µg (%)
p = 0.009
p = 0.0001
p = 0.0001
NT CLQ
F
Control CRISPR
IRE1α CRISPR
Area (µm²)
p = 0.0001
IRE1α : WT KO
CRISPR
Circularity
p = 0.049
WT KO
CRISPR
G
CRISPR IRE1α
+Mock
+IRE1α -HA
ROI1
ROI2
Time(s): 0 10 20 30
Mock
IRE1α -HA
Num. Triple points/area
Time (s)
p = 0.004
IRE1α -HA: + -
CR IRE1α
Branch lenght (µm)
Time (s)
Branch length (µm)
IRE1α -HA: + -
CR IRE1α
H
IRE1α KO
IRE1α-HA
Mock
Cristae width (A.U.)
p = 0.043
IRE1α-HA: + -
IRE1α KO
I
CRISPR
Control
IRE1α
Cristae width (A.U.)
p = 0.008
IRE1α: WT KO
CRISPR
J
MAM/ all mito peirmeter (%)
ΣMAM length (x1+x2)
Σmito perimeter (y1+y2+z1+z2)
(Cosson et at.. 2012)
MAM length (%)
MAM length (x1)
mito perimeter (y1)
(Stoica et at.. 2016)
K
Control CRISPR
IRE1α CRISPR
MAM length (%)
0.0005
IRE1α: WT KO
CRISPR
MAM / all mito. perimeter
0.0003
WT KO
CRISPR

Supplementary Figure 2

Altered mitochondrial bioenergetics in IRE1α deficient cells.

(A) ATP measurement in the indicated cell lines with a luminescence assay (n = 18 biologically independent samples). **(B)** Indicated cell lines imaged using AT01 cytosolic FRET probe. Scale bar = 20 µm (total cells analysed: Mock: n = 91 cells; IRE1α-HA: n = 62 cells). **(C)** Indicated cells were processed for WB analysis to measure pAMPK followed by quantification using total AMPK (dashed line indicated spliced gel to avoid irrelevant lanes) (n = 6 biologically independent samples). **(D)** Indicated cells were imaged for LC3-II immunofluorescence and confocal microscopy after 6 h treatment with or without 2 h pre-exposure to starvation (CLQ = 1 µM chloroquine, BAF = 0.1 µM bafilomycin A_1). Right panel: LC3-II dot count per cell were quantified (n = 3 independent experiments; total cells analysed from left to right: 67; 89; 65; 99; 70; 91; 80; 91; 51; 103; 69; 96). Scale bar = 20 µm). **(E)** ATP determination of cells described in B with the indicated treatments after 24 h of 1 µM CLQ (n = 17 biologically independent samples). **(F)** Same cells as in E imaged with TEM. Scale bar = 4 µm. Graph bars representing the area and circularity for the indicated conditions (control: n = 55 cells; IRE1α: n = 60 cells). **(G)** Live imaging of CRISPR IRE1α KO cells transiently expressing KDEL-RFP with IRE1α-HA or Mock. Graph bars represent the mean for the indicated parameter (n = 3 independent experiments, Scale bar = 10 µm). **(H-I)** Indicated cells were imaged with TEM. Scale bar = 200 nm. Distance between *cristae* was determined (total mitochondria analysed: Mock: n = 36; IRE1α-HA: n = 35; Control: n = 32; IRE1α: n = 32). **(J)** Summary of two different approximations to quantify MAM length. **(K)** ER longitudinal contact distance (red arrows) was measured by the 2 approaches described in J (n = 3 independent experiments). Scale bar = 500 nm. (Total events analysed: CRISPR control: n = 17 contacts; CRISPR IRE1α: n = 28 contacts). All plots represent mean and SEM. Unpaired or paired (K) Student´s t-test was used. Source data have been provided in Supplementary Table 6.

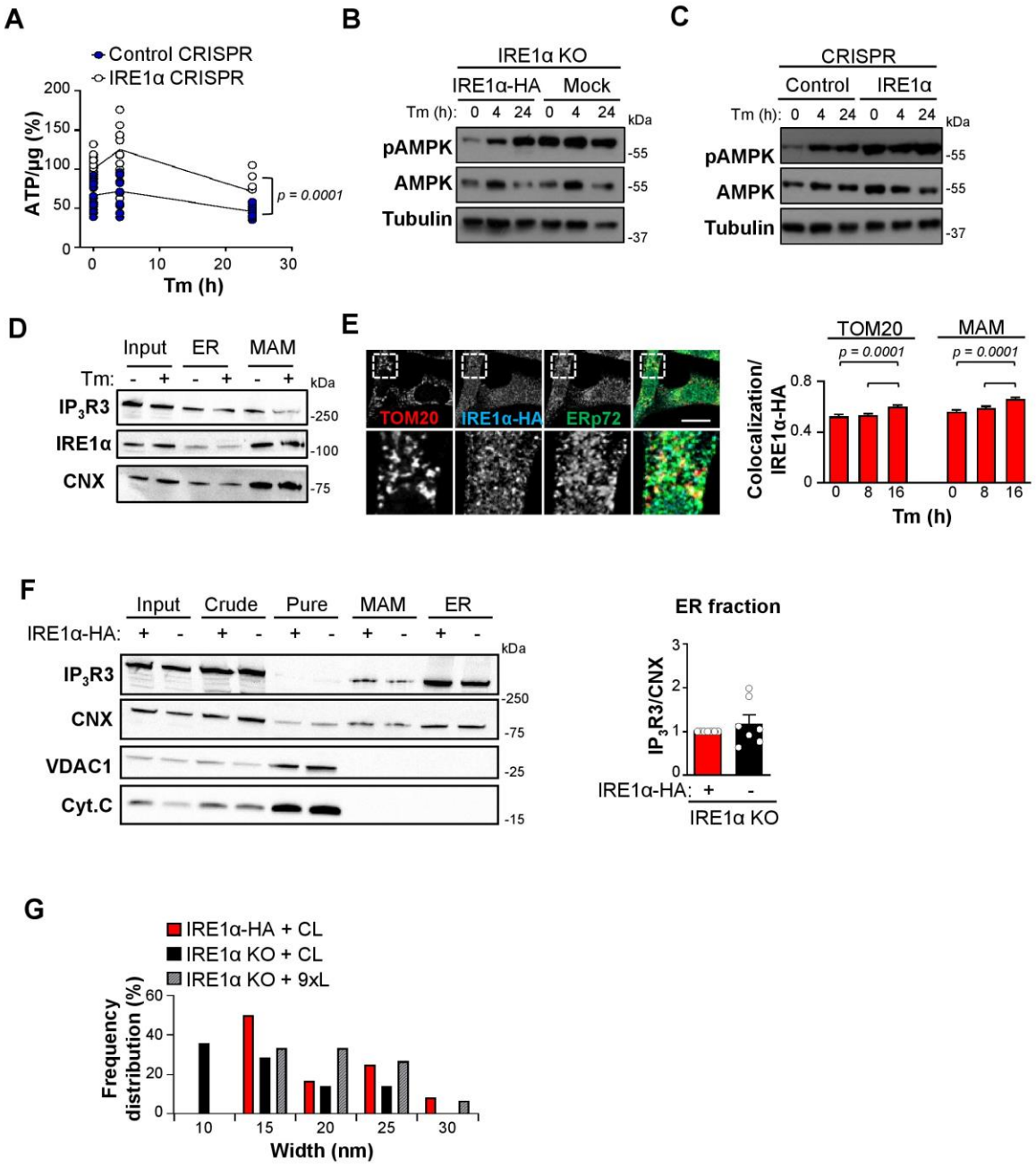

Supplementary Figure 3

IRE1α modulates mitochondrial bioenergetics under ER stress.

(A) ATP measurements in cells treated with 100 ng/ml tunicamycin (Tm) for the indicated times (NT: n = 18; 4h: n = 12; 24h: n = 8; all n are biologically independent experiments). **(B)** IRE1α KO cells reconstituted with IRE1α-HA or Mock or CRISPR cells **(C)** were processed for western blot analyses to monitor levels of indicated proteins. Cells were treated with 100 ng/ml Tm for the indicated times (n = 3 independent experiments). **(D)** IRE1α KO cells were reconstituted with IRE1α-HA and processed to obtain purified MAM fractions after 4 h treatment with 1 µg/ml Tm. Fractions were analysed by western blot (WB) for indicated UPR and MAM markers (Cr: crude mitochondria; H: homogenate; M: MAMs; P: pure mitochondria; C: cytosol; E: ER) (n = 2 independent experiments). **(E)** Same cells described in D were treated with 0.1 µg/ml Tm for indicated time points and stained for ERp72, TOM20 and HA using indirect

immunofluorescence. Scale bar = 20 µm. Confocal microscopy analysis and co-localization coefficient was calculated (n = 3) (total cells analysed for t = 0 and 16; n = 40; t = 8; n = 43). **(F)** IRE1α KO cells reconstituted with IRE1α-HA or empty vector (Mock) were processed to obtain subcellular fractions and analysed by WB to monitor the levels of indicated proteins. Right panel: quantification in the expression of IP_3R3 normalized to calnexin (CNX) in the ER fraction (n = 6 independent experiments). **(G)** IRE1α KO cells reconstituted with IRE1α-HA or empty vector (Mock) transiently expressing control or 9x MAMs linker were imaged for TEM to measure MAMs width. Graph represents the frequency distribution of MAMs width. All plots represent mean and SEM. Statistical differences were detected with unpaired Student´s t-test; two-way ANOVA (A). Source data have been provided in Supplementary Table 6.

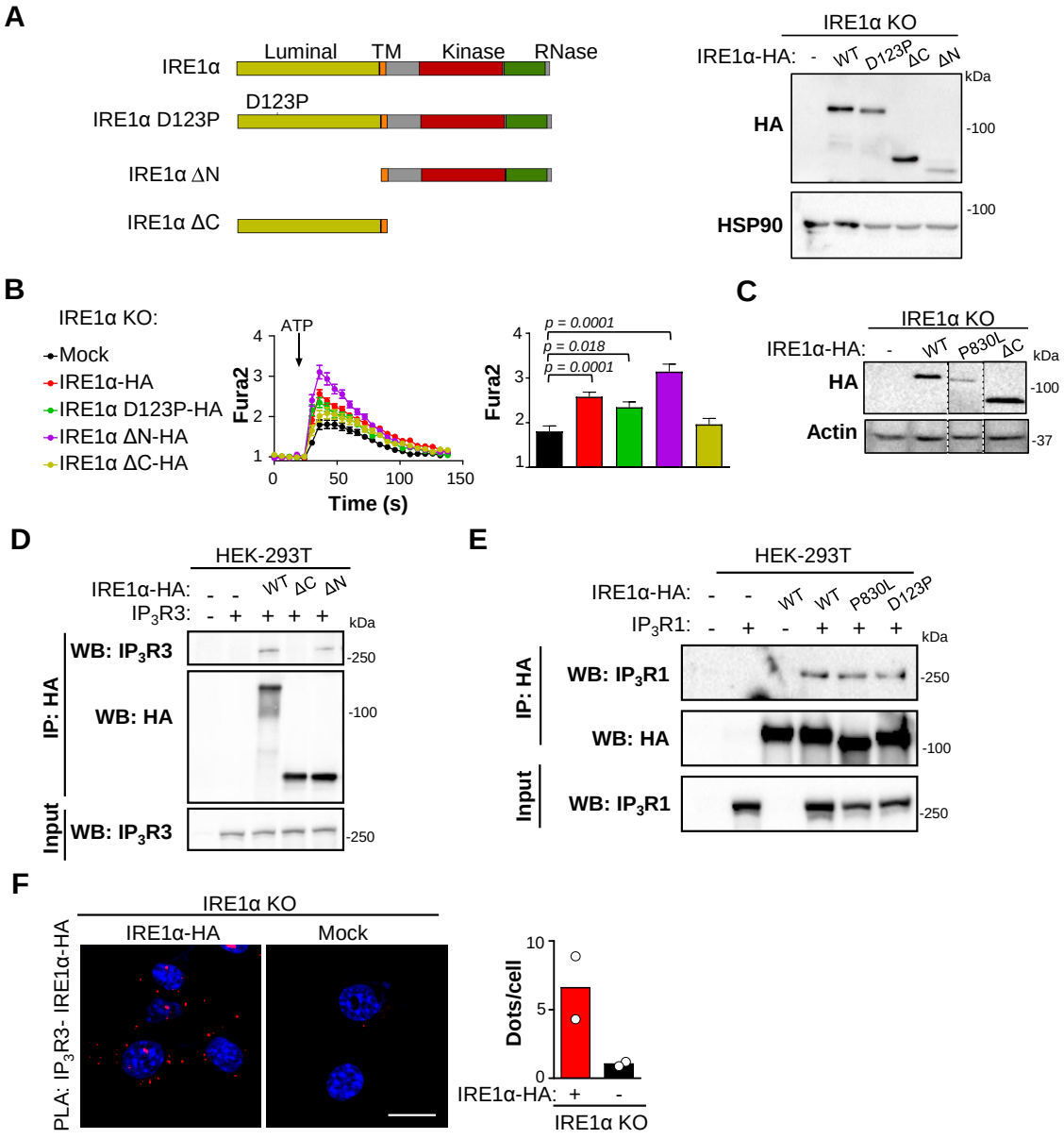

Supplementary Figure 4

IRE1α physically interacts with IP_3R1.

(A) Left: scheme representing IRE1α structure and the different mutants used, including D123P, a deletion of the entire cytosolic region and a deletion of the entire N-terminal region. Right panel: cells stably expressing designated constructs described in were processed for western blot analysis to measure levels of indicated proteins (n = 3 independent experiments). **(B)** Left panels: IRE1α KO cells reconstituted with the indicated constructs were imaged for calcium levels in the cytosol (Fura2-AM) in a calcium free media (n = 4). Arrow = stimulation with 100 µM ATP. Right panel: The maximum peak for normalized Fura2-AM ratio is presented (total cells analysed: Mock: n = 99 cells; IRE1α-HA: n = 109 cells; IRE1α-D123P-HA: n = 78 cells; IRE1α-ΔN-HA: n = 92 cells and IRE1α-ΔC-HA: n = 91 cells). **(C)** IRE1α KO cells reconstituted with empty vector (Mock), IRE1α-HA, IRE1α-P830L-HA, or IRE1α-ΔC-HA were processed for western blot (WB) analysis to monitor the levels of indicated proteins. Dashed lines indicate cropped gels to eliminate irrelevant lanes from the same image (n = 2 independent experiments). **(D)** and **(E)** HEK 293T cells were transiently transfected with

indicated constructs and immunoprecipitated (IP) with an anti-HA antibody. WB analysis was performed for the indicated proteins in IPs and total input (n = 2 independent experiments). **(F)** IRE1α KO cells reconstituted with IRE1α-HA or Mock were stained with PLA using antibodies to detect IP_3R3 and VDAC1 proteins. Right panel: mean number of dot counts per cell were quantified (n = 2 independent experiments). All plots represent mean and SEM. Statistical differences were detected with ANOVA and Dunnett's multiple comparison test. Source data have been provided in Supplementary Table 6.

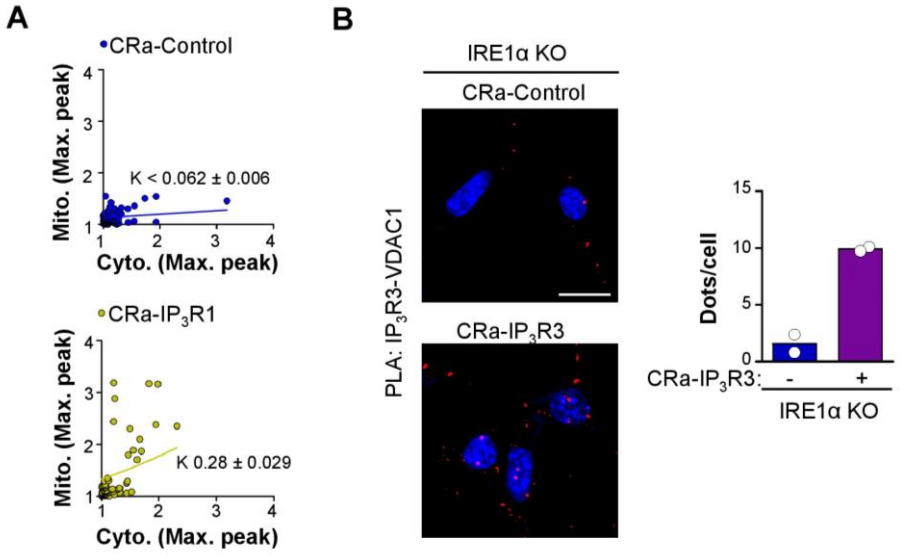

Supplementary Figure 5

Enhanced expression of IP_3R1 reverts the defects in calcium signalling observed in IRE1α null cells.

(A) IRE1α KO cells stably expressing CRa-IP_3R1 or CRa-Control were imaged for calcium in the cytosol and mitochondria simultaneously with Fura2-AM and Rhodamine2N-AM (Rhod2). Integration of the maximum peak of individual cells from Fura2-AM and Rhod2-AM signals to calculate the non-linear regression k value and SEM (n = 5 independent experiments; total cells analysed: CRa-IP_3R1: n = 87 cells; CRa-Control: n = 65 cells). **(B)** CRa-IP_3R3 or CRa-Control were stained for proximity ligation assay (PLA) with anti-IP_3R3 and anti-VDAC1 antibodies and visualized by confocal microscopy. Scale bar = 10 µm. Right panel: mean dots per cell were quantified (n = 2 independent experiments). Source data have been provided in Supplementary Table 6.

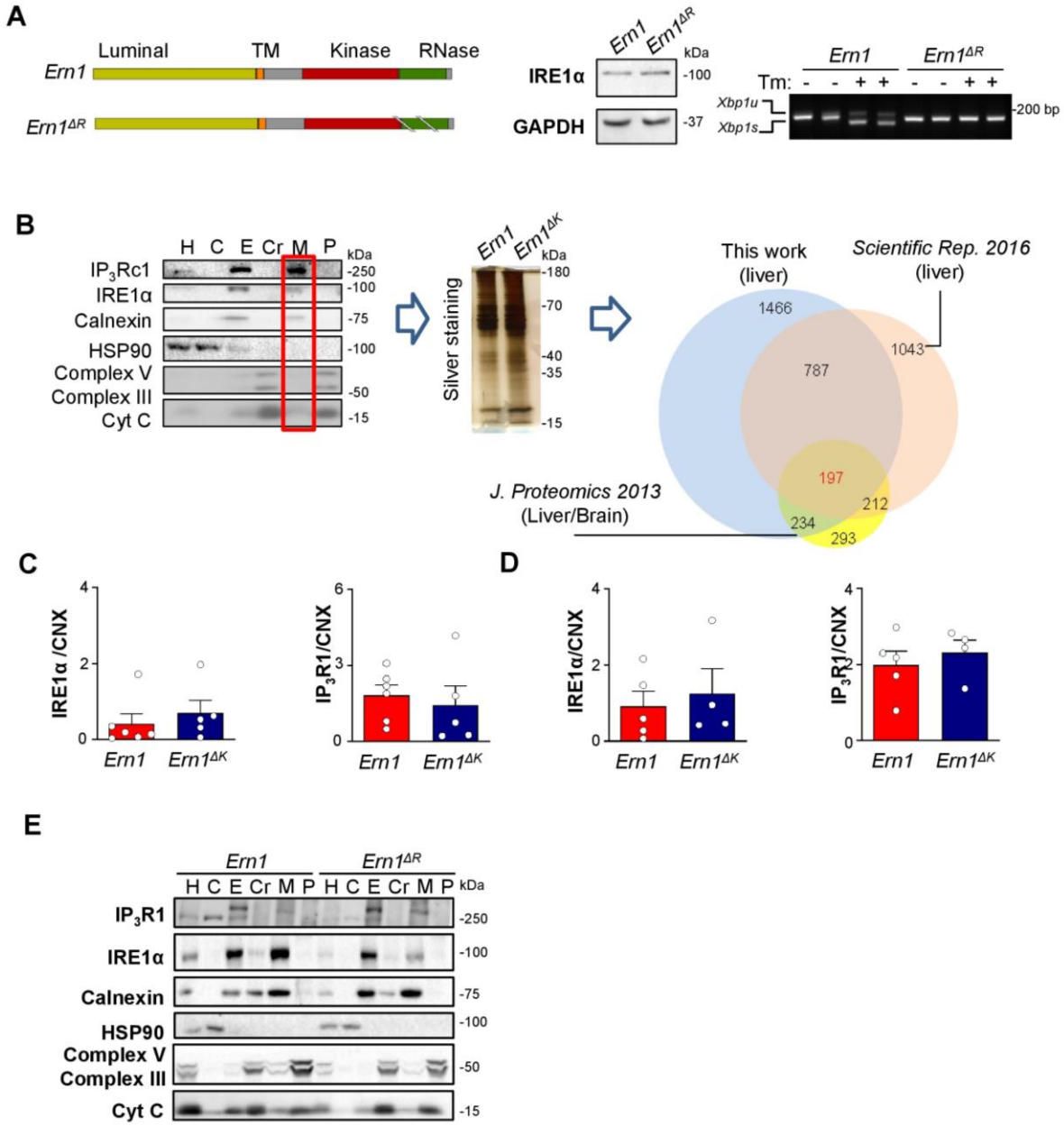

Supplementary Figure 6

IRE1α regulates MAMs biology *in vivo*.

(A) Upper panel: scheme representing *Ern1* structure and deletion strategy (*Ern1*$^{\Delta R}$). Down, left: livers from *Ern1* and *Ern1*$^{\Delta R}$ processed for WB for the indicated proteins. Western blot (WB) is representative of a minimum of three independent experiments. Bottom panel, right: *Ern1* and *Ern1*$^{\Delta R}$ mice were intraperitoneally injected with 1 mg/Kg tunicamycin (Tm) or vehicle for 6 h and then *Xbp1* mRNA splicing was evaluated by RT-PCR (n = 2 independent experiments). **(B)** Illustration of the flow chart of the MAMs proteomics. Left: representative WB of wild-type liver subcellular fractionation highlighting the MAMs fraction. Middle: silver staining of representative MAMs fractions. Right: Venn diagram representing the intersections between the hits obtained in the MAMs proteomics of this study, with two other studies, (related to Tables S3-S4). **(C-D)** Indicated liver samples were processed to obtain subcellular fractions and analysed by WB against the indicated antibodies. **(C)** Total extracts (*Ern1* n = 6 animals; *Ern1*$^{\Delta K}$ n = 5 animals). **(D)** ER fraction (*Ern1* n = 5 animals; *Ern1*$^{\Delta K}$ n = 4 animals). **(E)** Indicated liver samples were processed to obtain subcellular fractions and analysed by WB for

the indicated markers (Cr: crude mitochondria; H: homogenate; M: MAMs; P: pure mitochondria; C: cytosol; E: ER) Representative WB of n = 3 animals. All plots represent mean and SEM. Source data have been provided in Supplementary Tables 3 and 4.

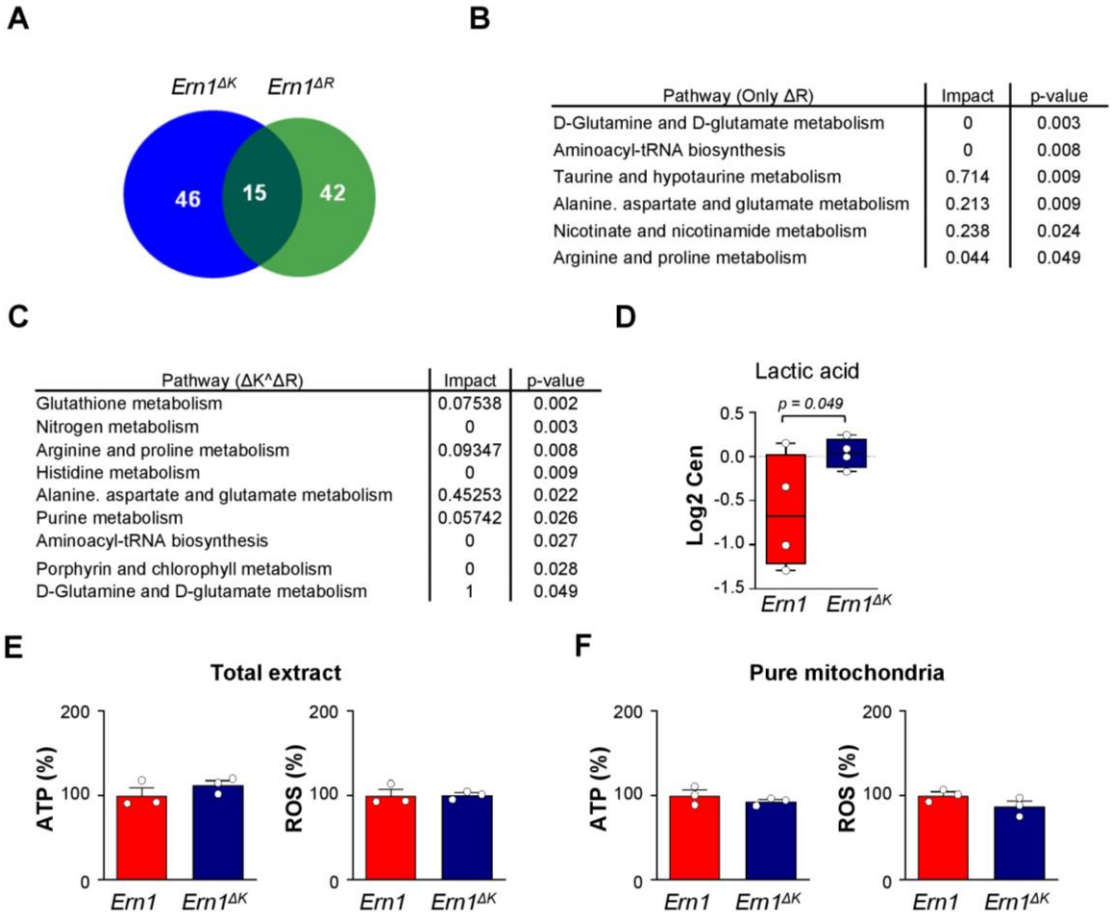

Supplementary Figure 7

IRE1α regulates cellular metabolism *in vivo*.

(A) Venn diagram for metabolomics data showing the overlap in metabolites altered in *Ern1*$^{\Delta K}$ and *Ern1*$^{\Delta R}$. **(B-C)** Pathway impact probability and significant alterations in metabolites calculated with MetaboanalystR from Table S5. **(B)** Altered pathways only in *Ern1*$^{\Delta R}$ (n = 3 animals per group). **(C)** Altered pathways only in *Ern1*$^{\Delta R}$ and *Ern1*$^{\Delta K}$ intersection (n = 3 and 4 animals per group, respectively)**. (D)** Complement to figure 7A-D: Whiskers and dot plots of indicated metabolites comparing *Ern1* and *Ern1*$^{\Delta K}$ liver samples (4 animals per group). **(E-F)** *Ern1* control and *Ern1*$^{\Delta K}$ liver samples were processed to obtain total tissue homogenates (E) and isolated mitochondria (F) and analysed for mitochondrial respiration (ATP levels) and ROS production (n = 3 animals per group). Statistical differences were detected with one (D) or two –tailed (B-C) Student´s t-test. Source data have been provided in Supplementary Table 5.

Figure 1

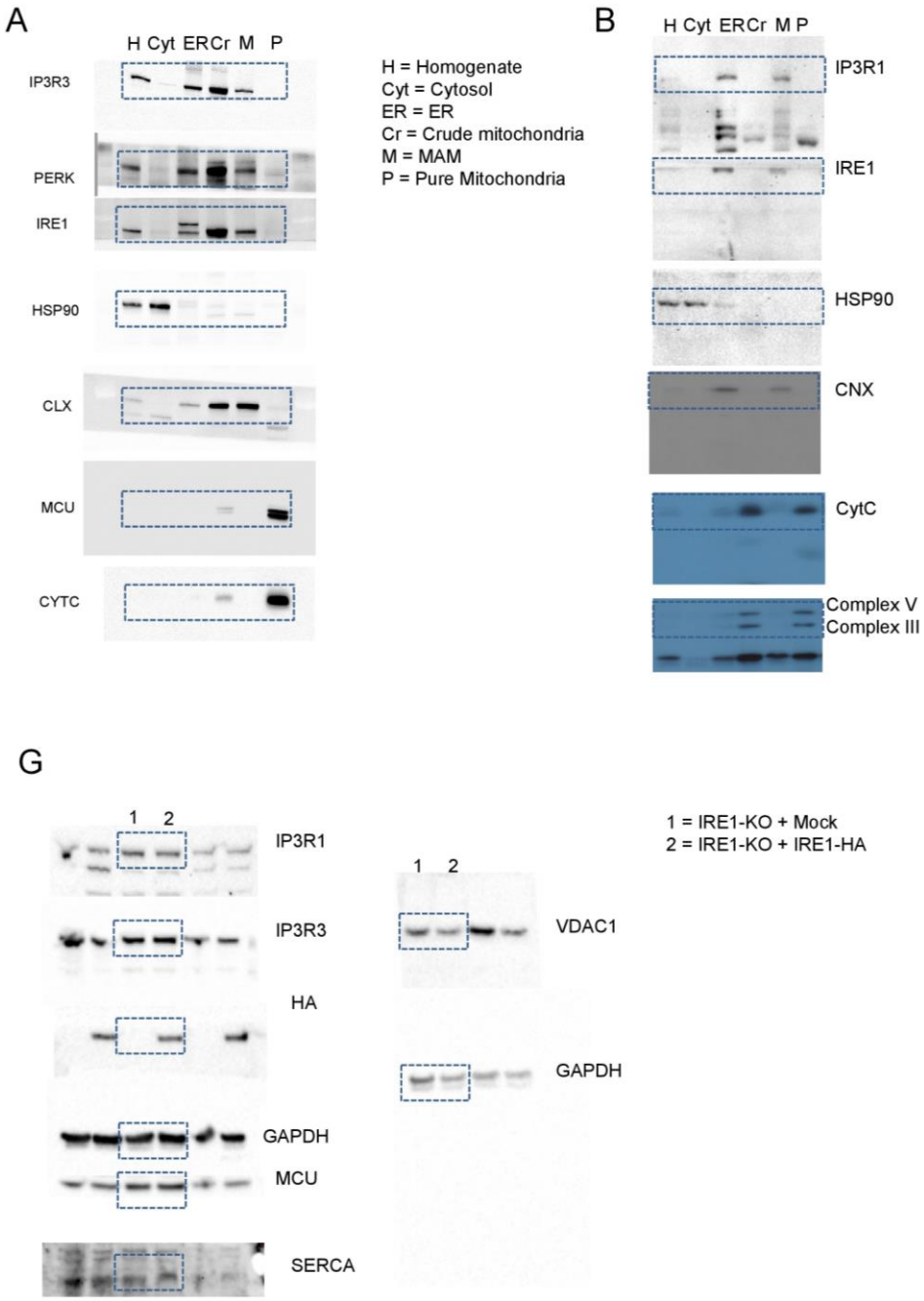

Supplementary Figure 8

Unprocessed images of all gels and blots

All gels and blots presented in this work are displayed unprocessed and labeled. The name of the main figure and panel corresponds to the processed images presented in the final manuscript. Specific lanes are indicated with a blue dashed line.

Figure 2

I

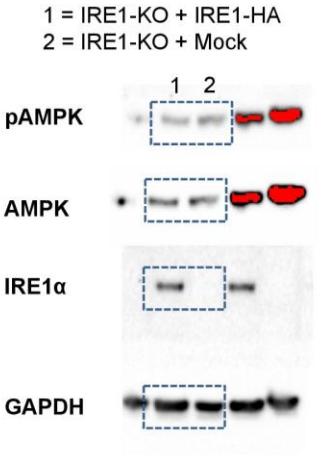

J

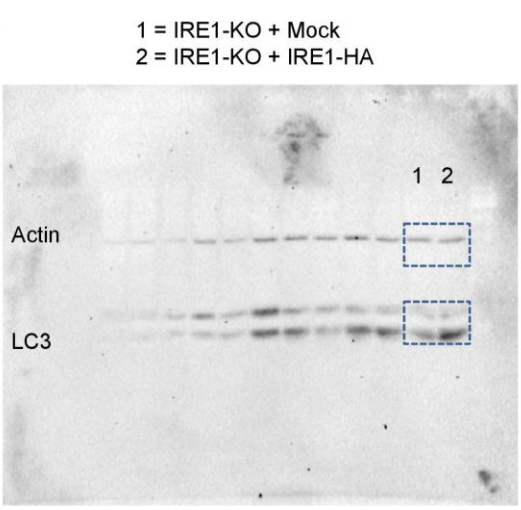

Figure 3

A

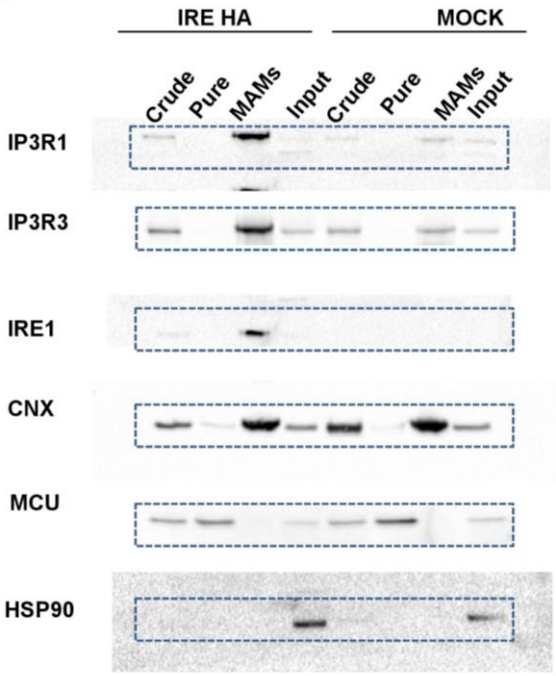

Supplementary Figure 8

Continued

All gels and blots presented in this work are displayed unprocessed and labeled. The name of the main figure and panel corresponds to the processed images presented in the final manuscript. Specific lanes are indicated with a blue dashed line.

Figure 4

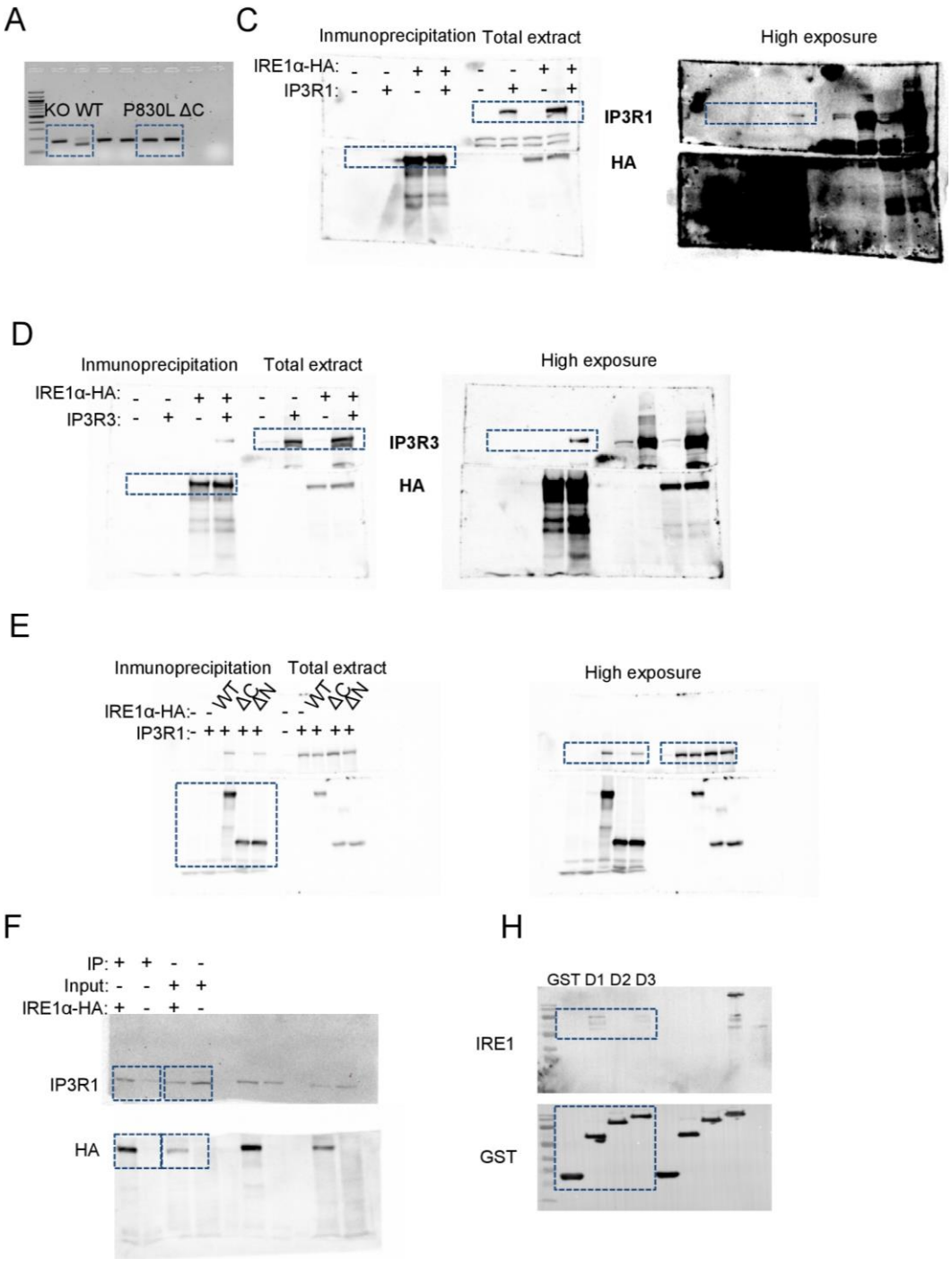

Supplementary Figure 8

Continued

All gels and blots presented in this work are displayed unprocessed and labeled. The name of the main figure and panel corresponds to the processed images presented in the final manuscript. Specific lanes are indicated with a blue dashed line.

Figure 5

A

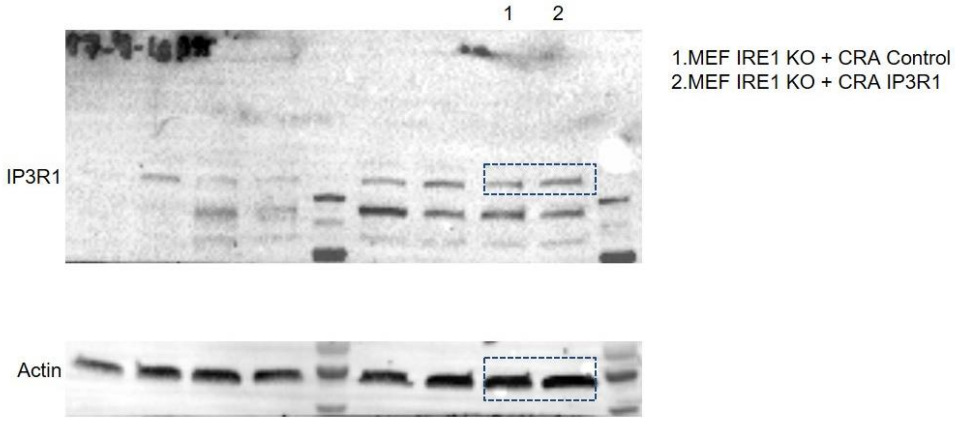

E

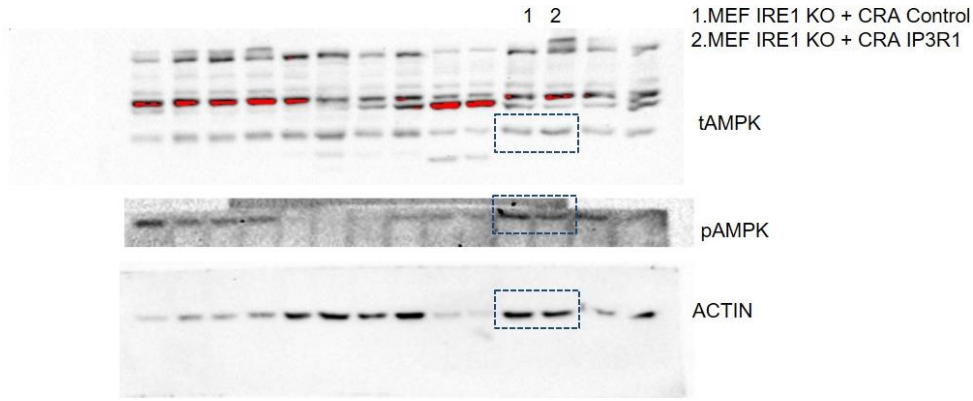

G

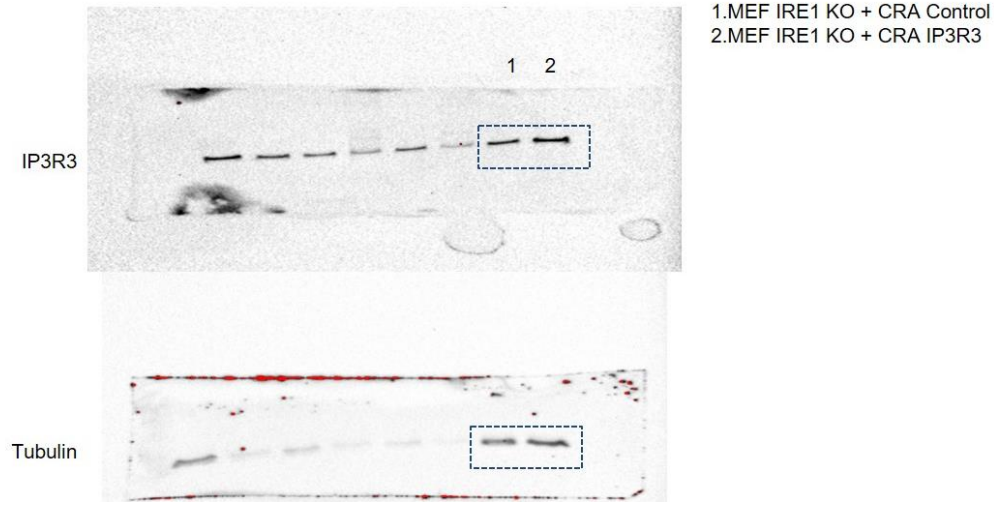

Supplementary Figure 8

Continued

All gels and blots presented in this work are displayed unprocessed and labeled. The name of the main figure and panel corresponds to the processed images presented in the final manuscript. Specific lanes are indicated with a blue dashed line.

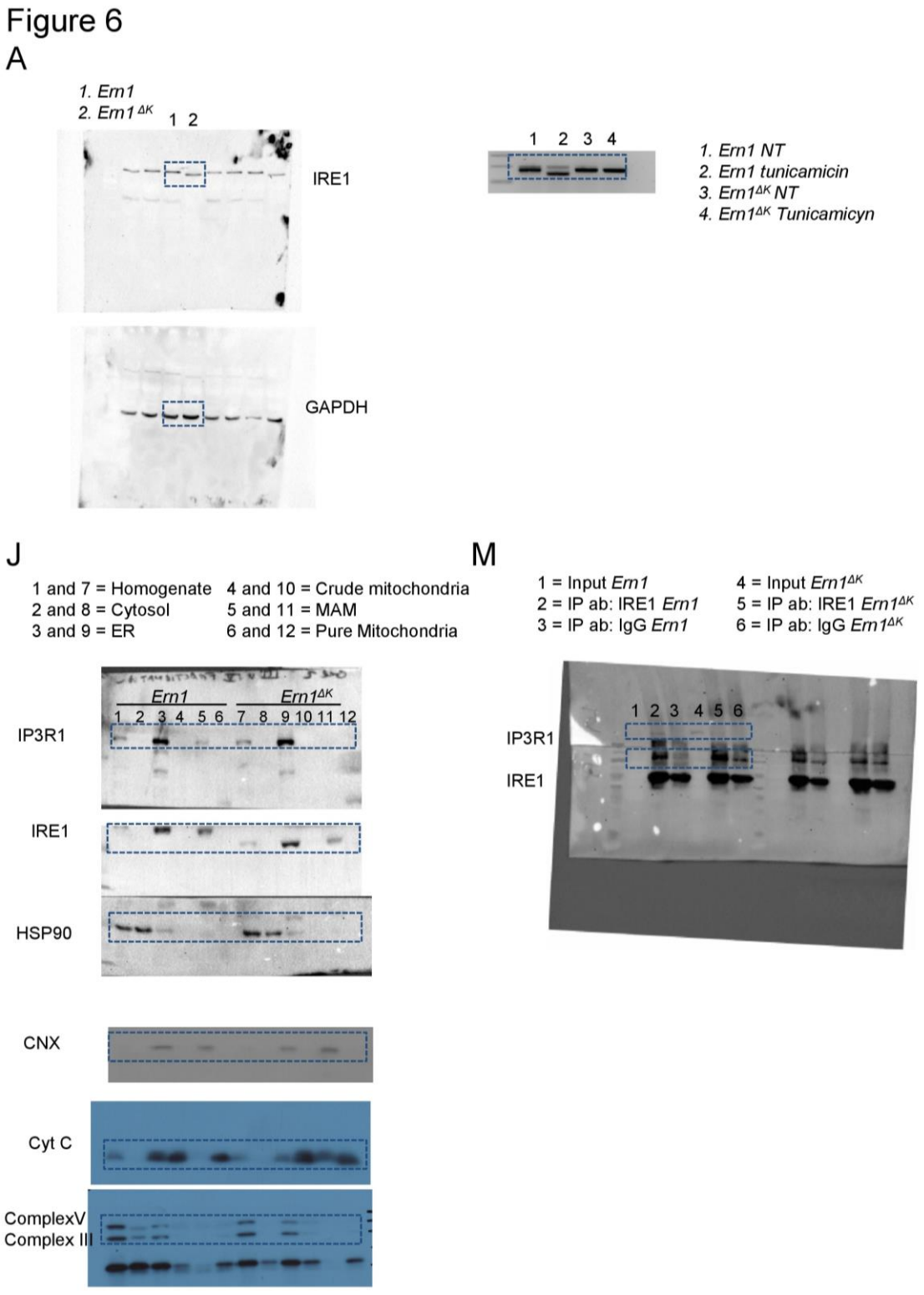

Supplementary Figure 8

Continued

All gels and blots presented in this work are displayed unprocessed and labeled. The name of the main figure and panel corresponds to the processed images presented in the final manuscript. Specific lanes are indicated with a blue dashed line.

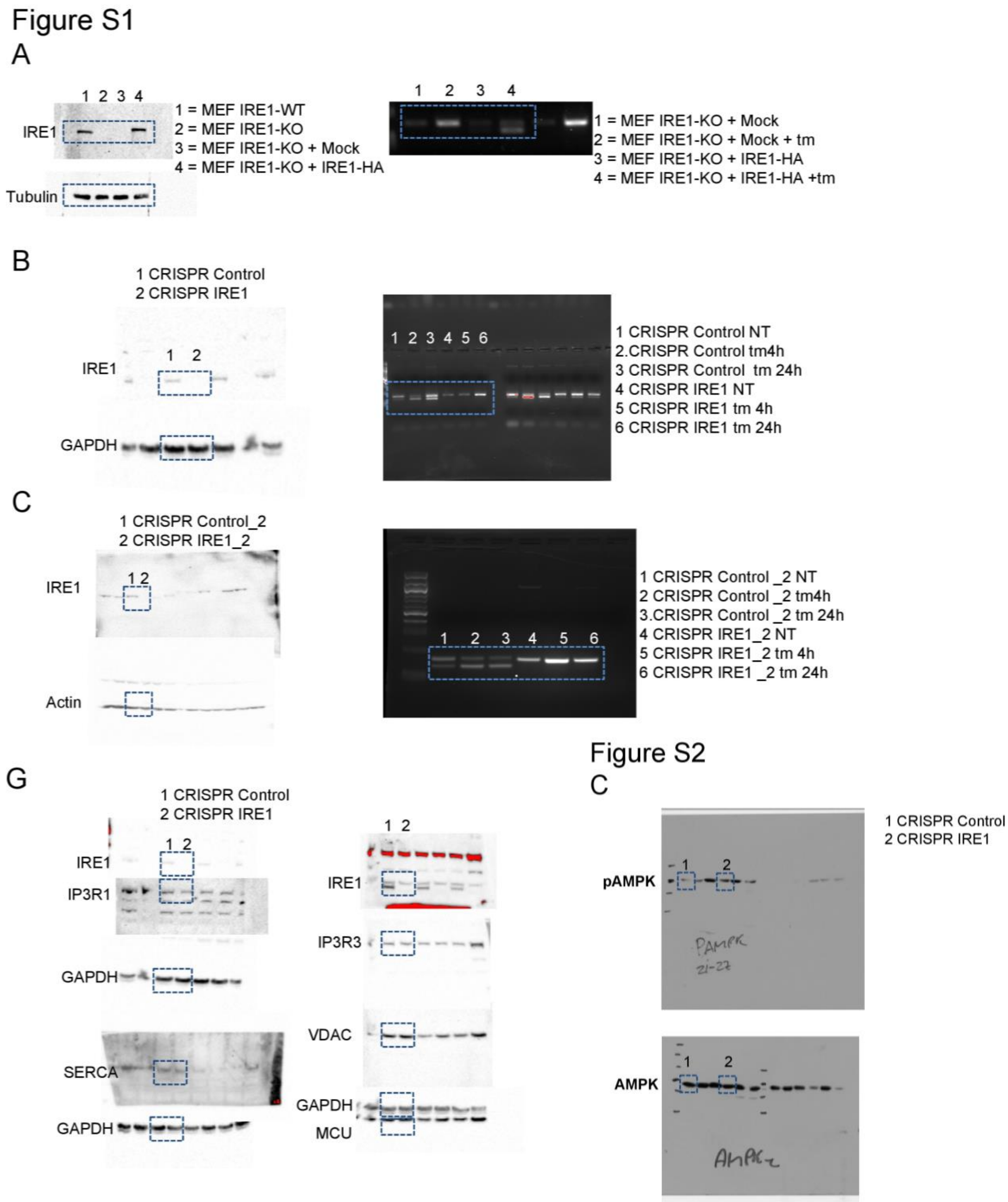

Supplementary Figure 8

Continued

All gels and blots presented in this work are displayed unprocessed and labeled. The name of the main figure and panel corresponds to the processed images presented in the final manuscript. Specific lanes are indicated with a blue dashed line.

Figure S3

B

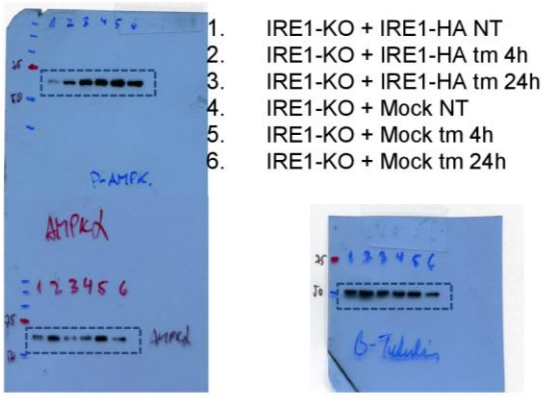

1. IRE1-KO + IRE1-HA NT
2. IRE1-KO + IRE1-HA tm 4h
3. IRE1-KO + IRE1-HA tm 24h
4. IRE1-KO + Mock NT
5. IRE1-KO + Mock tm 4h
6. IRE1-KO + Mock tm 24h

C

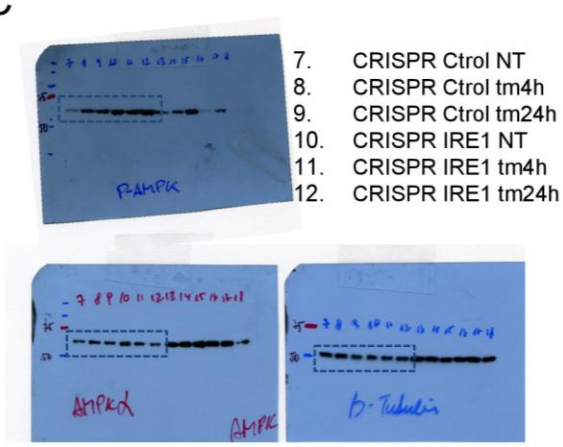

7. CRISPR Ctrol NT
8. CRISPR Ctrol tm4h
9. CRISPR Ctrol tm24h
10. CRISPR IRE1 NT
11. CRISPR IRE1 tm4h
12. CRISPR IRE1 tm24h

D

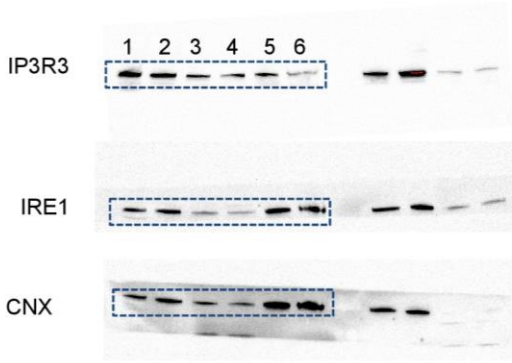

1. INPUT - IRE1-KO + IRE1-HA NT
2. INPUT - IRE1-KO + IRE1-HA + Tm 4h
3. ER - IRE1-KO + IRE1-HA NT
4. ER - IRE1-KO + IRE1-HA + Tm 4h
5. MAMs - IRE1-KO + IRE1-HA NT
6. MAMs - IRE1-KO + IRE1-HA + Tm 4h

F

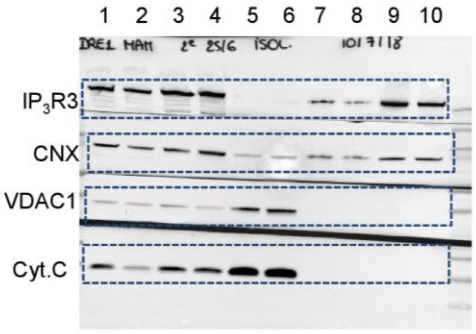

1. INPUT - IRE1-KO + Mock
2. INPUT -IRE1-KO + IRE1-HA
3. Mito-Crude - IRE1-KO + Mock
4. Mito-Crude - IRE1-KO + IRE1-HA
5. Mito-Pure - IRE1-KO + Mock
6. Mito-Pure - IRE1-KO + IRE1-HA
7. MAMs - IRE1-KO + Mock
8. MAMs - IRE1-KO + IRE1-HA
9. ER - IRE1-KO + Mock
10. ER - IRE1-KO + IRE1-HA

Supplementary Figure 8

Continued

All gels and blots presented in this work are displayed unprocessed and labeled. The name of the main figure and panel corresponds to the processed images presented in the final manuscript. Specific lanes are indicated with a blue dashed line.

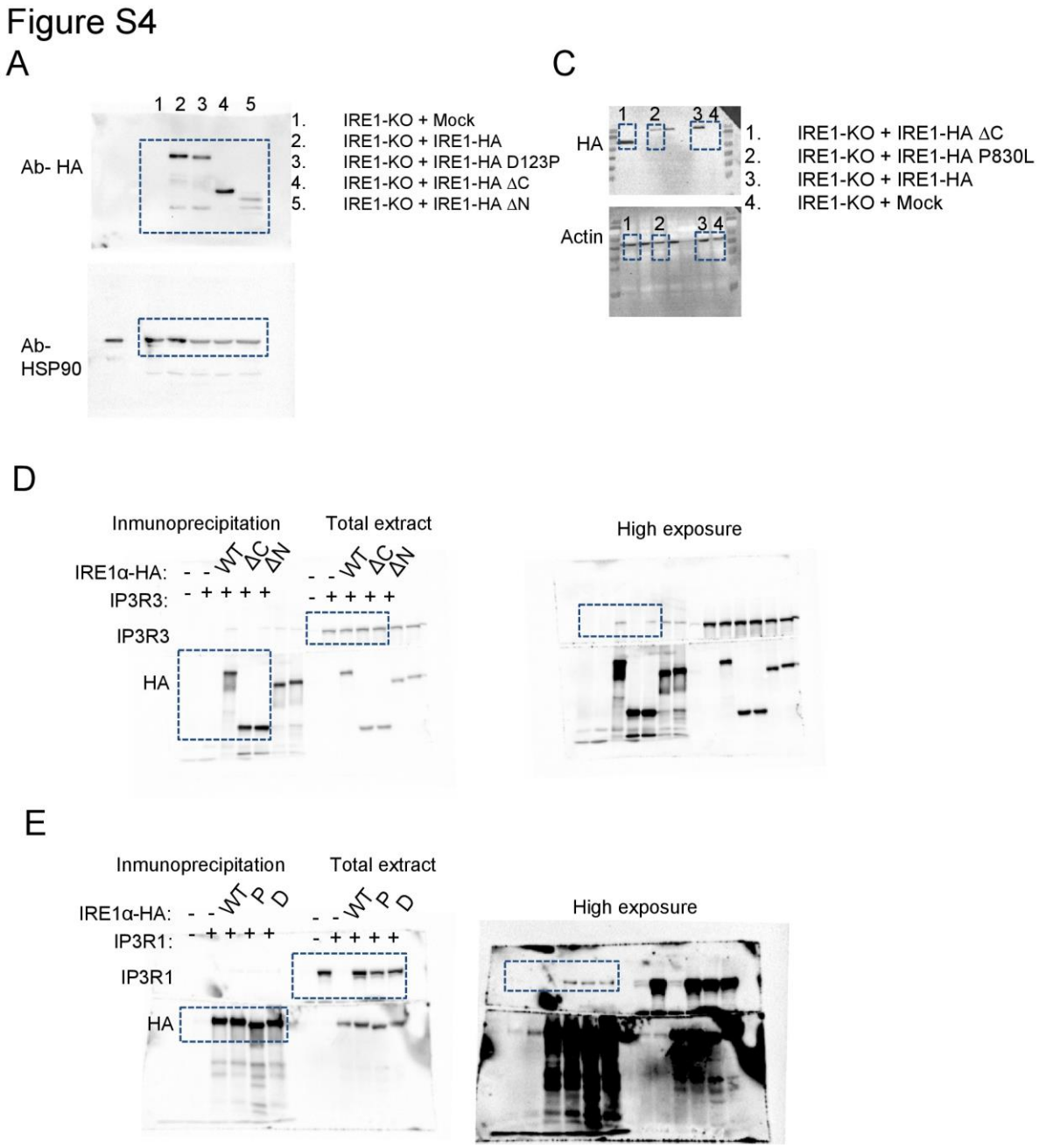

Supplementary Figure 8

Continued

All gels and blots presented in this work are displayed unprocessed and labeled. The name of the main figure and panel corresponds to the processed images presented in the final manuscript. Specific lanes are indicated with a blue dashed line.

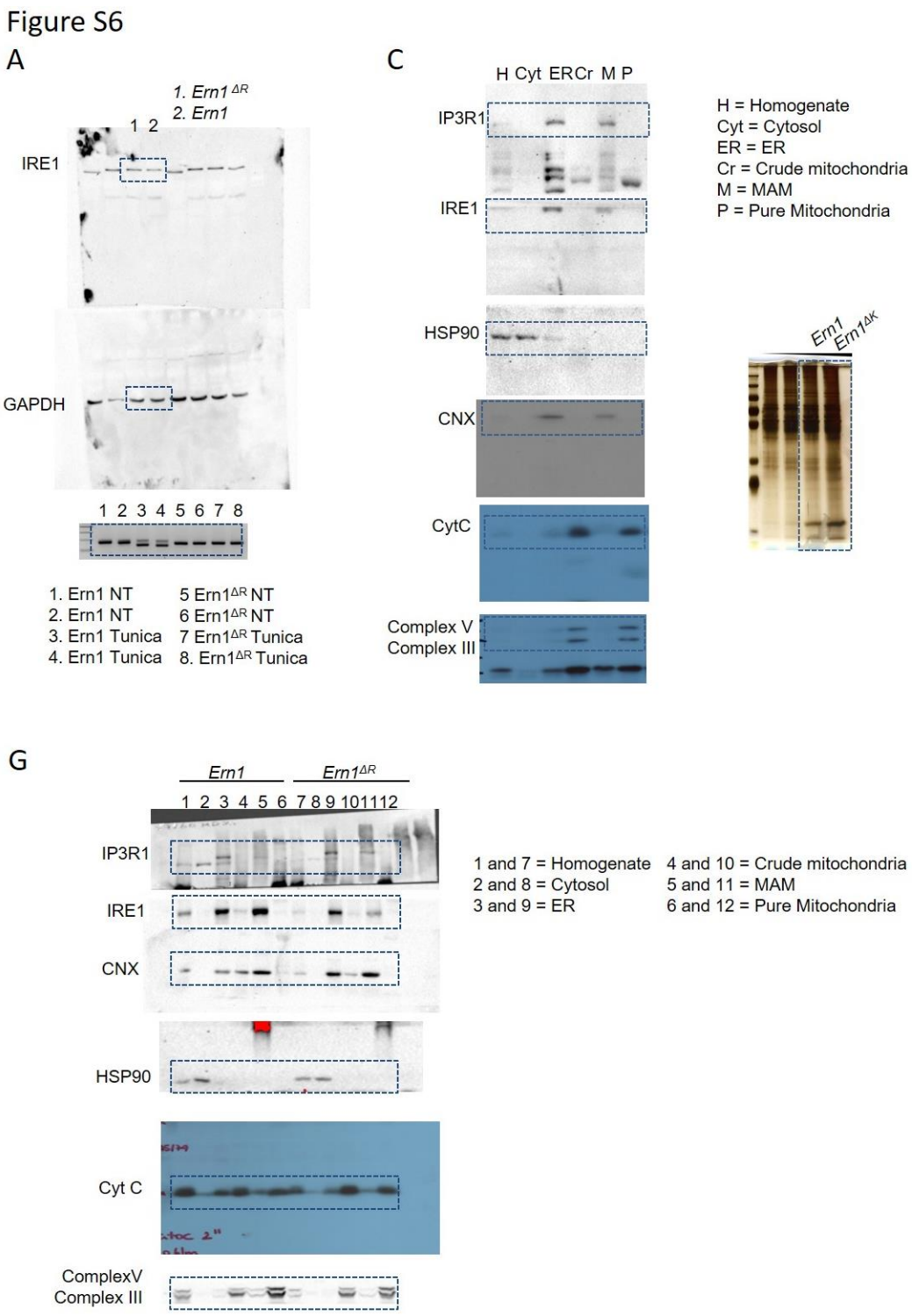

Supplementary Figure 8

Continued

All gels and blots presented in this work are displayed unprocessed and labeled. The name of the main figure and panel corresponds to the processed images presented in the final manuscript. Specific lanes are indicated with a blue dashed line.

Supplementary Table 1. ER morphological parameters. Morphological ER parameters obtained from TEM imaging based on *Cosson et al.* Analysis for 3 independent experiments. Mean and SEM are displayed. Statistics were calculated using unpaired two tailed Student-t test.

Supplementary Table 2. **MAMs morphometric values**. Morphometric values obtained for every individual TEM experiments. Data presentation is based on *Cosson et al* analysis. Related to Figure S2K. Data is the mean value for 3 independent experiments.

Supplementary Table 3. MAM total protein list. Proteomic hits obtained from quantitative proteomics of purified MAMs presented on Figure 6H. N = 3 animals per group. Unpaired two tail Student t test was applied.

Supplementary Table 4. MAMs consensus proteins. Identification of all hits on different proteomic screenings of MAMs proteins (including this study). Significant hits in the consensus MAMs final set of proteins presented in Figure 6I are highlighted in green. Intersections for every column to obtain Venn diagram on Figure S6B.

Supplementary Table 5. Metabolomics data. Set of hits of significantly altered metabolites comparing *Ern1*$^{\Delta R}$ and *Ern1*$^{\Delta K}$ mice liver samples compared to each WT mice (n = 3 and 4 animals per group, respectively). Related to Figure S7A-C. Significance was calculated using unpaired Student t test.

Supplementary Table S6. Statistics source data. Statistics source data are provided for Figures 1-7 and for Supplementary Figures S1-S4 and S7. All statistics of this work organized by panel and figure. Indicated the type of test, mean, N, error and p value for the specified test.